Three-Dimensional Observation of Phase-Separated Poly(Methyl Methacrylate)/Poly(Styrene-*ran*-4-bromostylene) Blends by 3D NMR Microscopy with X-ray Microscopy

Satoshi Koizumi,[1] Yuji Yamane,[1] Shigeki Kuroki,[1] Isao Ando,[1] Yukihiro Nishikawa,[2] Hiroshi Jinnai[2]

[1]*Department of Chemistry and Materials Science, International Research Center of Macromolecular Science, Tokyo Institute of Technology, Ookayama, Meguro-ku, Tokyo 152-8552, Japan*
[2]*Department of Polymer Science, Kyoto Institute of Technology, Matsugasaki, Sakyo-ku, Kyoto 606-8585, Japan*

Received 1 December 2005; accepted 23 April 2006
DOI 10.1002/app.24952
Published online in Wiley InterScience (www.interscience.wiley.com).

ABSTRACT: Three-dimensional (3D) image patterns of phase-separated poly(methyl methacrylate) (PMMA)/poly (styrene-*ran*-4-bromostyrene) (PS-Br) blends heated at 180°C for 6, 8, and 10 h were observed by 3D NMR microscopy with 3D X-ray microscopy in order to characterize the 3D structure of the polymer blends using a standard 3D reconstruction protocol program for obtaining the 3D digital array of the PS-Br/PMMA morphologies. The phase-separated structure of the polymer blends in several 10-μm scales was reasonably characterized. The phase-separated structure of polymer blends by 3D NMR images was quantitatively consistent with that by 3D X-ray images. It can be said that 3D NMR microscopy is a very useful means for analyzing the 3D structure of phase-separated polymer blends as well as 3D X-ray images. © 2006 Wiley Periodicals, Inc. J Appl Polym Sci 103: 470–475, 2007

Key words: three-dimensional structure; NMR imaging; 3D NMR microscopy; 3D X-ray microscopy; phase-separated PMMA/PS-Br blends

INTRODUCTION

It has been demonstrated that NMR imaging is a very useful means for obtaining nondestructively μm-scale spatial information on probe molecules in bulk matters with μm-scale cavities.[1,2] For this, NMR imaging has been successfully used to elucidate the stimulus-response process of polymer gels under the application of external stimuli, such as stress, heating, and electric field, the transportation of probe metal ions in a polymer gel under electric field, and the number of channel cavities and its size distribution in a polymer gel.[3–11]

Studies of bicontinuous structures developed via spinodal decomposition (SD) have been a research theme among researchers dealing with binary mixtures of molecular fluids, binary alloys, and polymer blends.[12,13] Scattering techniques such as light, small-angle X-ray, and small-angle neutron have been extensively used to examine the phase-separated structure of polymer blends.[13–15] As a result of these studies, a great deal of information on the time evolution of the phase-separated structures has been obtained. Most recently, laser scanning confocal microscopy (LSCM) was shown to be an excellent tool to capture the 3D interface structure of polymer blends.[16–18] By using LSCM, the time evolution of the interface between two coexisting phases developed via SD was quantitatively captured in 3D images. At present, high-resolution X-ray computed tomography (X-ray CT) was also developed and it will be possible to provide very useful quantitative information about the μm-scale 3D structures of polymer blend systems; the mechanism of phase separation for polymer blends has been clarified.

In the X-ray CT method, the contrast of images comes from the difference of absorption for X-ray, which corresponds to the difference of electron density. Polymers have almost the same absorption for X-ray. If polymer blends are observed by X-ray CT, heavy atom-labeling is necessary for contrast enhancement. In the case of LSCM, the labeling of fluorescence species is necessary for contrast enhancement.

On the other hand, in ^{1}H NMR microscopy the contrast of images comes from the difference of ^{1}H spin density, ^{1}H spin-lattice relaxation time (T_1), and ^{1}H spin-spin relaxation time (T_2). Here, the difference of T_1 and T_2 corresponds to the difference in molecular motion. Thus, one does not need to label any specified

Correspondence to: S. Kuroki (skuroki@polymer.titech.ac.jp).

species for doing contrast enhancement for the observation of polymer blends. Nevertheless, to our best knowledge, there is no application to investigate phase-separated structures of polymer blends using 3D NMR microscopy.

Thus, we aim to carry out several 10 μm-scale 3D structural characterizations of phase-separated poly (styrene-*ran*-4-bromostyrene)/poly(methyl methacrylate) blends by 3D NMR microscopy, and to clarify the potential of 3D NMR microscopy as one of the methodologies for analyzing several 10 μm-scale 3D structures of polymer blend systems by comparing the observation of the same polymer blend samples by means of 3D X-ray CT. Further, the features of 3D NMR microscopy will be clarified.

EXPERIMENTAL

Sample preparation

A blend of poly(styrene-*ran*-4-bromostyrene) (PS-Br) and poly(methyl methacrylate) (PMMA) was used in the present study. PS-Br is made by bromination[19] of phenyl rings of polystyrene (PS), purchased from Japan Polystyrene (Tokyo, Japan). The bromination of PS is necessary for contrast enhancement for X-ray CT. A molar-average degree of bromination is 0.28 that is determined by elemental analysis (a potentiometric titration). PMMA is purchased from Sumitomo Chemical (Tokyo, Japan). The weight-average molecular weight (M_w) and polydispersity (M_w/M_n, where M_n denotes the number-average molecular weight) of PS-Br are 1.4×10^5 and 2.36, respectively. M_w and M_w/M_n for PMMA are 6.0×10^4 and 2.31, respectively.

A mixture of PS-Br and PMMA (PS-Br/PMMA = 50/50 wt%) was dissolved in benzene to form 5% homogeneous solution and then lyophilized. The mixture after lyophilization was melt-pressed at 180°C and molded into a disk shape of 5 mm in diameter and 5 mm in thickness. During this molding process, phase separation between PS-Br and PMMA occurs. Three different phase-separation times of the PS-Br/PMMA mixtures are employed at 6, 8, and 10 h. These are termed samples 1, 2, and 3, respectively. In this time range, phase separation is in the advanced stage. The PS-Br/PMMA mixtures after the heating treatment are then quenched by placing them on a metal plate that is cooled in liquid N_2. The optical microscope observation of samples 1, 2, and 3 was made as shown in Figure 1. It is seen from this figure that phase separation is advanced with thermal treatment time at 180°C. However, the optical microscope observation cannot provide nondeconstructively the 3D structural information.

For the observation of 3D ^{1}H NMR images with a high resolution of several 10 μm, the PS-Br/PMMA mixtures are washed with acetonitrile to solute only PMMA-rich domains. These samples are put into a flask and the flask is decompressed and then water is

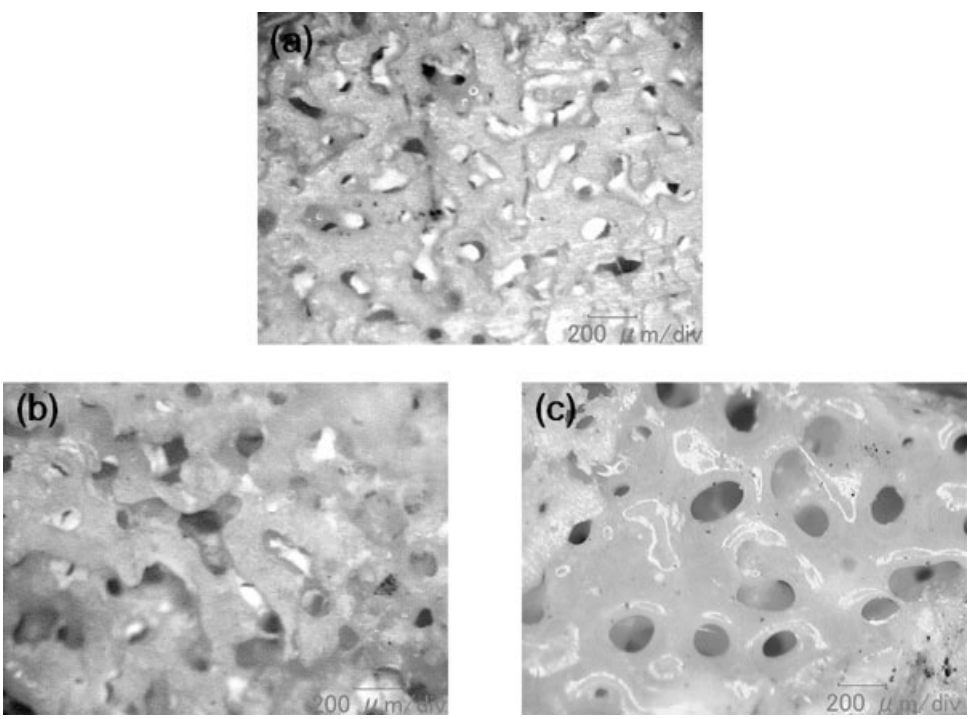

Figure 1 The observed optical microscope photographs of phase-separated PS-Br/PMMA blend samples 1 (a), 2 (b), and 3 (c) with thermal treatment times of 6, 8, and 10 h, respectively, at 180°C.

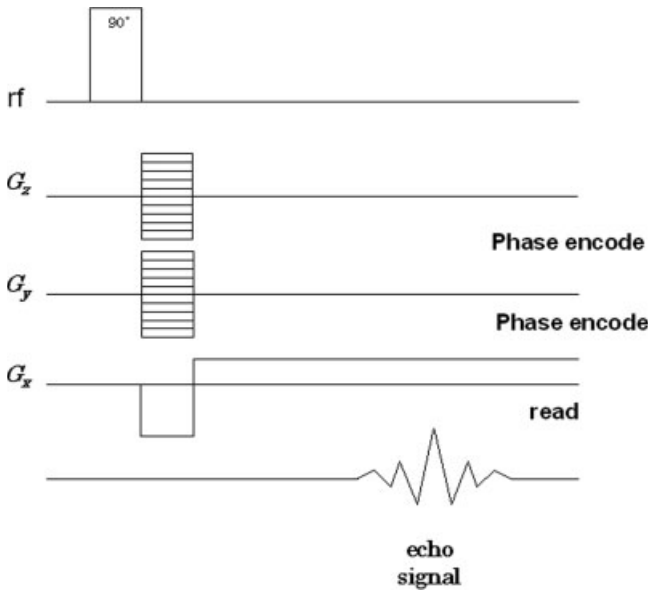

Figure 2 A pulse sequence of the 3D gradient echo method used in this work.

poured into the flask in order to replace the space that has been PMMA-rich domains with water.

3D NMR imaging measurements

The 3D ^{1}H NMR images of these samples were observed with a Bruker (Billerica, MA) Avance 300 spectrometer operating at 300 MHz with an imaging system with a maximal gradient strength of 100 mT/m at room temperature. The imaging pulse sequence is based on the 3D gradient echo (GE) pulse sequence,[20] shown in Figure 2. In the 3D GE method, the field gradients in the y and z directions (G_y and G_z) are the phase-encoding gradient, while the field gradient in the x direction (G_x) is the frequency-encoding gradient. The flip angle is 30°, the repetition time (TR) is 1 s, and the echo time (TE) is 3.771 ms.

The data processing of the 3D images was performed by 3D Fourier transform (FT). For the acquisition and processing of NMR data, the ParaVision program supplied by Bruker was used.

X-ray CT measurements

The 3D observations of the PS-Br/PMMA mixtures were performed with X-ray microtomography instruments (Elescan, Nittesu, Japan). The principles and basic instrumentation are described elsewhere.[21] The X-ray source was operated at 40 kV. The magnification was 16.7. A high precision rotating stage with an air bearing was used for rotating the sample. A series of X-ray absorption images (''projections'') were acquired over 180° in 0.2° increments with a CCD camera (C7300, Hamamatsu Photonics K. K., Japan, 1280 × 1000 pixels) equipped with an image intensifier. The background noise of the detector system, the so-called ''dark image,'' was subtracted from the projections. Subsequently, the image intensity in each

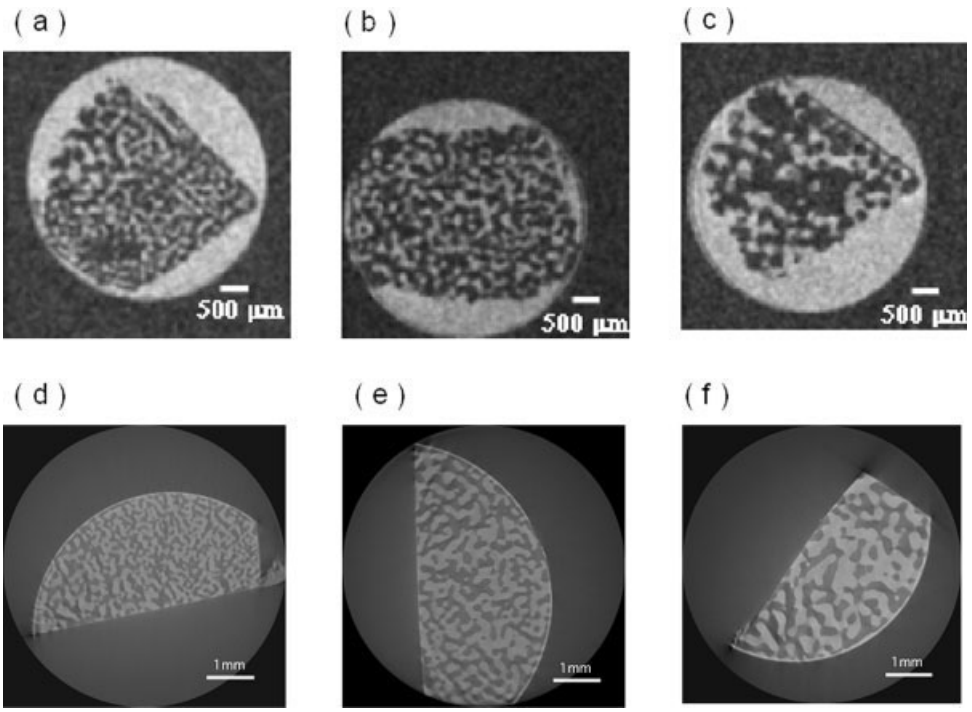

Figure 3 The observed XY-plane slice images of 3D ^{1}H NMR images (a–c) and X-ray CT (d–f) of phase-separated PS-Br/PMMA blends. The thermal treatment time was 6 h for (a) and (d), 8 h for (b) and (e), and 10 h for (c) and (f) at 180°C.

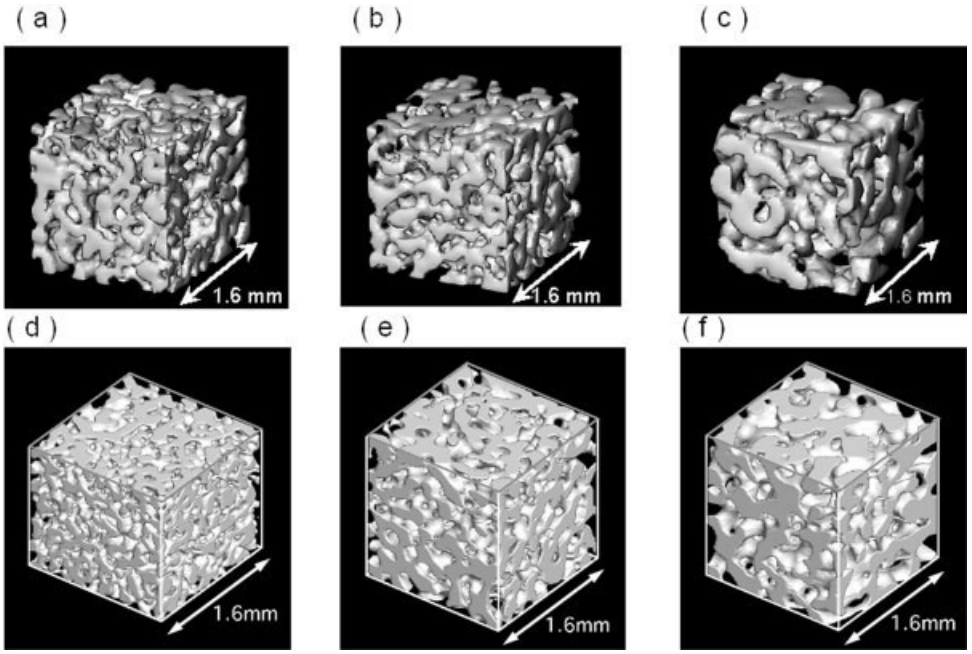

Figure 4 The observed 3D images reconstructed by the 2D NMR images (a–c) and X-ray CT (d–f) datasets. The thermal treatment time was 6 h for (a) and (d), 8 h for (b) and (e), and 10 h for (c) and (f) at 180°C.

pixel was corrected by the precalibrated detector sensitivity and the spatial variation of X-ray illumination. Thus, the projections obtained were processed by the filtered back projection method[22] to obtain tomograms of the blend, which are stacked together to generate 3D digital array data. The speckle noises in the 3D digital array were eliminated by a median filter.[23] The 3D data processing was binarized to find the interface between PS-Br-rich and PMMA-rich domains according to a protocol previously described.[24]

RESULTS AND DISCUSSION

The observed 2D sliced ^{1}H NMR images of PS-Br/PMMA mixture as melt-pressed at 180°C at three different thermal treatment times, 6, 8, and 10 h, are shown in Figure 3(a–c), where the XY-plane sliced images are shown with a thickness of 40 μm in Z direction. In this experiment, only ^{1}H signals from water that exists in spaces that have been PMMA-rich domains are observed. Therefore, the bright regions correspond to spaces that have been PMMA-rich domains. The dark regions in these images correspond to spaces of PS-Br-rich domains. The 2D sliced transmission X-ray CT images are also shown in Figure 3(d–f), where the bright regions correspond to the spaces of PS-Br-rich domains. It was found that the scale width of both the PMMA-rich and PS-Br-rich domains increases as the treatment times increase in both the NMR and X-ray CT images.

In Figure 4(a–c) the 3D NMR images are shown of a PS-Br/PMMA mixture reconstructed by the XY-plane sliced images shown in Figure 3(a–c), where the bright

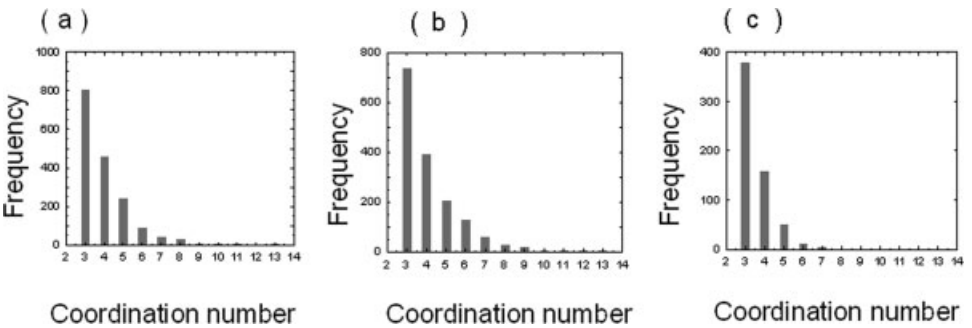

Figure 5 The distribution of the branch structure for a bicontinuous structure obtained by 3D NMR images. The thermal treatment time is 6 h for (a), 8 h for (b), and 10 h for (c) at 180°C.

TABLE I
Structural Parameters of the Size of Phase Separation Domain (Λ_m), the Volume Fraction of PS-Br($\Phi_{PS\text{-}Br}$) and the Surface Area per Unit Volume (S/V) and the Volume (V) Used as Calculated by the Observed 3D Datasets of 3D NMR Imaging and X-ray CT

Samples	Λ_m (μm)	$\Phi_{PS\text{-}Br}$	S/V (μm^{-1})	V (μm^3)
3D NMR imaging				
sample 1[a]	225	0.47	1.1×10^{-2}	9.3
sample 2[b]	278	0.46	1.0×10^{-2}	22.6
sample 3[c]	400	0.40	6.3×10^{-3}	14.1
3D X-ray CT				
sample 1[a]	222	0.50	1.5×10^{-2}	2.3
sample 2[b]	280	0.51	1.2×10^{-2}	7.1
sample 3[c]	376	0.51	9.3×10^{-3}	8.1

[a] Thermal treatment time of 6 h at 180°C.
[b] Thermal treatment time of 8 h at 180°C.
[c] Thermal treatment time of 10 h at 180°C.

and dark regions indicate PMMA-rich and PS-Br-rich domains, respectively. The data points are 128 × 128 × 128, and the voxel size is 40 × 40 × 40 μm. Figure 4(d–f) shows the 3D images reconstructed by the 2D transmission X-ray CT image datasets shown in Figure 3(d–f). The features of the 3D NMR images and 3D X-ray CT images are very close to each other. Also, they are very close to the optical microscope photographs shown in Figure 1.

It is well known that polymer blends of PMMA and PS take a bicontinuous structure in the phase separation process. Also, the bicontinuous structure of the PMMA-rich and PS-Br-rich domains can be nondestructively observed in both the 3D NMR and X-ray CT images shown in Figure 4. We made an animation video of the inner cavity of the blend sample and then analyzed the branch structure for all of the inner cavities. Figure 4 shows the animation video clip for the surface of the phase-separated blend samples. The scale width increases as the thermal treatment time increases. The μm-scale phase-separated structure of the PS-Br/PMMA blends is visually shown in Figures 3 and 4. It is shown that phase separation advances with the thermal treatment time.

The distribution of the branch structure for a bicontinuous structure obtained from 3D NMR images is shown in Figure 5, where the thermal treatment time is 6 h for (a), 8 h for (b), and 10 h for (c) at 180°C. As seen from this figure, the fraction that the bicontinuous structure takes three branches at each junction point is more than 50%. The average distribution of the branching number at the junction points is almost independent of the thermal treatment time in the present experiments.

The log-log plots of the integrated intensity(s(q)) versus q-space calculated by FT of both 3D NMR and X-ray CT images of PS-Br/PMMA blend samples are shown in Figure 5(a–c), where the thermal treatment time is 6 h for (a), 8 h for (b), and 10 h for (c) at 180°C. The overall shapes of s(q) for the 3D NMR imaging and X-ray CT results are very close to each other. The peak positions of these plots are connected with the characteristic wavelength of the PS-Br/PMMA phase-separated structure, which corresponds to the sizes of phase separation domains (Λ_m). Table I shows the sizes of phase-separated domains (Λ_m) calculated by the peak positions in Figure 6(a–c), the volume fraction of PS-Br ($\Phi_{PS\text{-}Br}$), the surface area per unit volume (S/V), and the volume (V) used in the calculation by 3D NMR imaging and X-ray CT. The Λ_m values of the PS-Br/PMMA blend samples at three different thermal treatment times, 6, 8, and 10 h, were 225, 278, and 400 μm, respectively, as determined by 3D NMR imaging. On the other hand, the corresponding Λ_m values as determined by X-ray CT were 222, 280, and 376 μm, respectively. The Λ_m values determined by 3D NMR imaging and 3D X-ray CT are very close to each other. The Λ_m increases as the thermal treatment time increases. Further, the $\Phi_{PS\text{-}Br}$ and S/V values obtained from 3D NMR and X-ray CT images are very close to each other. These results show that it is possible to quantitatively evaluate the phase-separated structure of polymer blends by using 3D NMR images as well as 3D X-ray CT images.

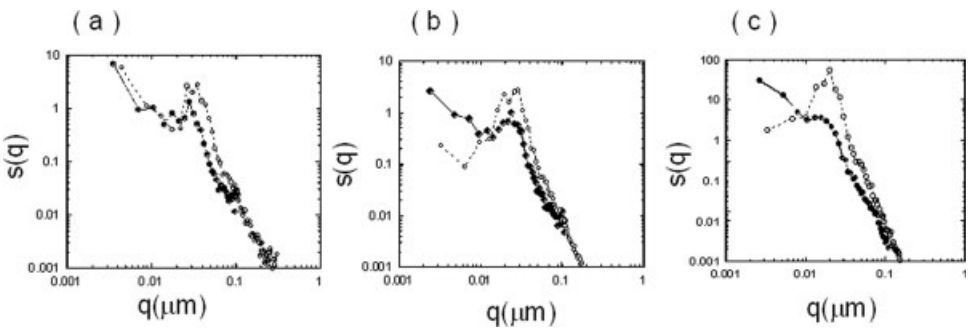

Figure 6 The plots of the integrated intensity versus q-space calculated by the FT of the observed 3D datasets. The thermal treatment time is 6 h for (a), 8 h for (b), and 10 h for (c) at 180°C. The filled black circles correspond to the 3D NMR imaging results, and the open white circles to the X-ray CT results.

CONCLUSIONS

The 3D NMR images of phase-separated PS-Br/PMMA blends were observed by 3D ^{1}H NMR microscopy and 3D X-ray CT. The bicontinuous structure of PS-Br-rich and PMMA-rich domains was successfully observed from both of two NMR imaging and X-ray CT measurements. The parameters for the size of phase separation domains, the volume fraction of PS-Br, and the surface area per unit volume as determined by the 3D NMR and X-ray CT images were very close to each other. From these experimental results it can be said that it is possible to quantitatively evaluate the phase-separated structure of polymer blends using 3D NMR images as well as 3D X-ray CT images.

References

1. Callaghan, P. T. Principles of Nuclear Magnetic Resonance Microscopy; Oxford University Press: Oxford, 1991.
2. Blümich, B. NMR Imaging of Materials; Clarendon Press: New York, 2000.
3. Yasunaga, H.; Kurosu, H.; Ando, I. Macromolecules 1992, 25, 6505.
4. Shibuya, H.; Yasunaga, T.; Kurosu, H.; Ando, I. Macromolecules 1995, 28, 4377.
5. Kurosu, H.; Shibuya, T.; Yasunaga, H.; Ando, I. Polymer J. 1996, 28, 80.
6. Yamazaki, A.; Hotta, Y.; Kurosu, H.; Ando, I. Polymer 1997, 28, 2082.
7. Yamazaki, A.; Hotta, Y.; H. Kurosu, I. Ando, Polymer 1998, 39, 1511.
8. Hotta, Y.; Shibuya, T.; Yasunaga, H.; Kurosu, H.; Ando, I. Polym Gels Netw 1998, 6, 1.
9. Yamazaki, A.; Hotta, Y.; Kurosu, H.; Ando, I. J Mol Struct 2000, 554, 47.
10. Hotta, Y.; Ando, I. J Mol Struct 2002, 602/603, 165.
11. Yamane, Y.; Koizumi, S.; Kuroki, S.; Ando, I. J Mol Struct 2005, 739, 137.
12. Gunton, J. D.; Miguel, M. S.; Sahni, P. S. In Phase Transition and Critical Phenomena; Domb, C.; Lebowitz J. L., Eds.; Academic Press: New York, 1983, p 269.
13. Hashimoto, T. Phase Transit 1988, 12, 47.
14. Hashimoto, T.; Takenaka, T.; Jinnai, H. J Appl Crystallogr 1991, 24, 457.
15. Jinnai, H.; Hasegawa, H.; Hashimoto, T.; Han, C. C. J Chem Phys 1994, 99, 8154.
16. Jinnai, H.; Nishikawa, Y.; Koga, T.; Hashimoto, T. Macromolecules 1995, 28, 4782.
17. Jinnai, H.; Koga, T.; Nishikawa, Y.; Hashimoto, T.; Hyde, S. T. Phys Rev Lett 2000, 84, 518.
18. Jinnai, H.; Nishikawa, Y.; Morimoto, H.; Koga, T.; Hashimoto, T. Langmuir 2000, 16, 4380.
19. Kambour, R. P.; Bendler, J. T. Macromolecules 1986, 19, 2679.
20. Adam, G.; Nolte-Ernsting, C.; Prescher, A.; Buhne, M.; Bruchmuller, K.; Kupper, W.; Gunther, R. W. J Magn Reson Imaging 1991, 1, 665.
21. Sasov, A.; Van Dyck, D. J. Microsc 1998, 191, 151.
22. Herman, T. G. Image Reconstruction from Projections, The Fundamentals of Computerized Tomography; Academic Press: San Francisco, 1980.
23. Wayne, N. An Introduction to Digital Image Processing; Prentice-Hall International: London, 1986.
24. Morgan, C. L. In Basic Principles of Computer Tomography; University Park Press: Baltimore, 1983, Chapter 5.